Journal of New Materials for Electrochemical Systems 18, 243-249 (2015)

Investigation on the Electrochemical Manipulation of Bio-Molecules in Glass Nanofluidic Channels

Kun Liu[1,*], Ming Hao[1], Donghui Meng[2], Xujie Wan[3], Songwen Xiao[4], Songgang Sun[1], Dongyang Wang[1] and Dechun Ba[1,†]

[1]School of Mechanical Engineering and Automation, Northeastern University, 3-11 Wenhua Rd., Shenyang, China, 110004, China
[2]Beijing Institute of Spacecraft Environment Engineering, Beijing 100094, China
[3]Beijing Institute of Aviation Materials, China Aviation Industry Group Co.LTD. , Beijing 100095, China
[4]Institute of High Energy Physics Chinese Academy of Sciences, 100049 Beijing 100049, China

Received: November 17, 2015, Accepted: November 25, 2015, Available online: December 15, 2015

Abstract: *As the size of microfluidic channel further shrinks to nanometer, the dimension is approximate to biomolecules as well as Debye length (DL). Great deals of phenomena which do not exist in the usual world will appear. The overlapping of electrical double layers (EDL) in the channel and the increasing of the viscosity are such good examples. All of these phenomena lead to the fundamental research such as colloid science, transport process and micro/nanoscale hydrodynamics. It demands more advanced technique for micro/nanoscale design and fabrication as the channels downing to nanometer scale. In this work, molecular dynamics was adopted to calculate the transport of proteins and water molecules in nanofluidic channels. New methods of nanochannel fabrication were developed based on glass substrate. Glass nanochips were achieved via ultraviolet lithography and wet chemical etching. The channel depth could be adjusted by controlling the etching time. Finally the scanning electron microscope (SEM) and surface profiler were used to characterize the shape and surface morphology of the nanochannel in detail. This study presents the feasibility of such design and fabrication methods, which gives an interesting exploration for the application of nanofluidic technology.*

Keywords: nanofluidics; biological chip; molecular dynamics; wet chemical etching

1. INTRODUCTION

Since nano channels are similar to macromolecules such as DNA and proteins in size, nanofluidic chip can be applied in such amazing applied areas as single biomolecule detection, separation and analysis, which has attracted much attention to carry out basic research of biochemistry about nanofluidics [1-7]. Nanofluidic channels show great potentials in many fields such as the single molecule detection, molecule filter sieve and DNA separation technology [8-12]. There will be surface charge in channel inner wall when the solutions flow through the channel due to the adsorption effect of charged particles to the channel wall. The Debye length reflects the action scope of electrostatic force in the solution, which is usually 1~100nm in aqueous solution. The electrostatic force generated by surface charge can go through the entire channel corresponding to Debye length. Meanwhile, the number of surface charge and ions is fairly the same because the ratio of the surface area of nanofluidic channel and volume is relatively large while the size of nanofludic channel is relatively small. According to Gouy-Chapman-Stern model the composition and migration characteristics of the ions are determined by the surface charge in nanofluidic channel [13-15].

Plecis et al [16] introduced a nanofluidic device that can be used to study the transport of molecules in the nanofluidic channel. Two parallel microfluidic channels are connected by the flow channel. When the moving time of a molecule from one end to the other is measured, the time of molecule going through the nanofluidic channel is determined. Kuo et al [17] connected the multilayer microfluidic channel by the nanofluidic membrane and controlled the transfer of the sample in the nanofluidic channel connecting the microfluidic channels. Daiguji et al studied the transport model and the migration properties of ions in the SiO_2 nanotubes of 5 μm

To whom correspondence should be addressed:
*Email: kliu@mail.neu.edu.cn , Phone: 86-24-8367-6945; Fax: 86-24-8368-0450
†Email: dchba@mail.neu.edu.cn , Phone: 86-24-8368-7618; Fax: 86-24-8368-0450

in length and 30 nm in diameter [18]. Karnik et al manipulated the migration of proteins molecules, K^+ and Cl^- ions in the nanofluidic channel by using the field-induced effect of the nanofluidic transistor and its circuit [19].

Microfluidic chip analysis system has been widely applied in the rapid, high throughput and low consumption analysis of biochemical samples [20-24]. When the channel size is reduced to nanometer scale, the sample consumption is further decreased. What's more, the performance of chemical analysis will also be significantly improved due to the size effect [25-26]. In recent years quite a few literatures have reported the study in nanofluidic chips including enrichment, mixing of biological samples, single molecule analysis, detection, transmission, manipulation, separation and screening of biomolecule such as DNA [27-30].

In this paper, according to the characteristics of ion separation based on nanofluidic diodes, we carried out the modeling and numerical simulation for the transport process of biomolecule and ions in glass channel. Then we fabricated the glass-based nanofluidic chips by the integration of wet chemical etching and room temperature sealing technology, explored suitable conditions of wet etching, studied the relations between etching time, channel depth and width. Finally nanoscale channels were characterized by reasonable equipment. In room temperature sealing, the sealing technique was explored to ensure the reliable encapsulation of the chips.

Totally, a simple and feasible method for the design and fabrication of glass-based nanofluidic chips is explored based on the research of electrochemical manipulation theory. It is helpful for the further optimization of the design scheme and fabrication process as well as has a potential impact on vitro diagnostics, genomics, proteomics and organic matter, etc.

2. CHANNEL DESIGN AND NUMERICAL SIMULATION

The ionic transportation in nanofluidic channels under unbalanced condition can be divided into four categories as conical nanotube, bipolar membrane, nanofluidic diode and nanofluidic dynatron. The uneven surface charge distribution is their common characteristics. The difference of surface charge density results in the transformation between electric energy, and chemical energy during the ionic transport process.

2.1. Design model

In nanofluidic channels, ion of solution, ion adsorbed on the inner channel walls and induced charges from an external electric field will influence electrostatic field and thus influence the mobility of biomolecules and ions. Under different surface charges gradient distribution, ionic concentration gradient distribution and channel depth, the influence of electrokinetic effects to EDL, the impact of solid-liquid interface to the adsorption/desorption of biomolecules and ions are considered, so are the diffusion mechanism of biomolecule and ion on channel surface.

Based on the field-induced effect of series additional gate electrode, biomolecules and ions can be manipulated by adjusting the distribution of surface charges, which results in the adjusting of ionic concentration and biomolecule mobility. Multistage manipulation can be realized by taking advantage of the gradient action of space multilayer grid electrode. In the case of the non-overlapping

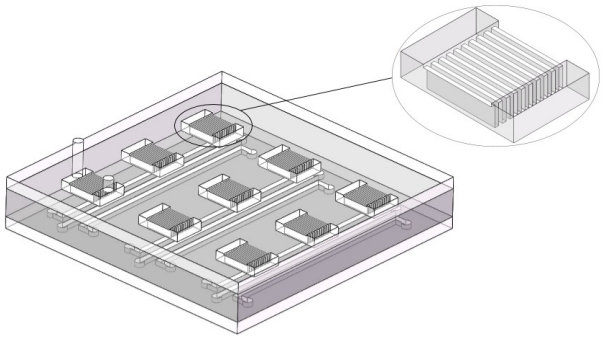

Figure 1. Design of nanofluidic chips

of EDL, ion current can be controlled through the surface electric charge density changed partially by grid electrodes. When the surface electric charge density of left part is the same as that of right part and both of symbols are contrary, nanofluidic diode will be formed. The nanofluidic transistor will be formed when the surface electric charge density changes in the middle section.

According to above theories, glass nanofluidic chips were achieved as shown in fig.1. From fig.1, nanofluidic chips were composed of several parts including glass substrate etched with nanometer scale channels, channel covering plate, liquid storage tank and rear electrode. The size details are as following: the length and depth of nanometer channel were 5mm and 50nm respectively. Width was defined as 2μm, 5μm and 10μm. For charges exiting on the channel walls, metal electrode need to be placed on the bottom of glass substrate. Metal electrode need to be lied under the channels uniformly, which was in favor of better controlling the charge distribution on the channel walls.

Nanofluidic diodes have shown the character of nanofluidic rectification in unbalanced condition. Nanofluidic diode can be effectively integrated with other nanofluidic devices and microfluidic devices through the rational design of nanofluidic diode. Nanofluidic diode or Nanofluidic devices can be applied in the pH control, electrolyte concentrations control and the separation process according to the analogy principle.

2.2. Numerical simulation

For micro and nano chips, the primary problem is the drive of micro and nano flow. To acquire rapid, stable and efficient driving modes for the movement of biomolecule in micro and nano channels, the flow driving modes in micro and nano chips and pressure-driven transfer characteristic of biomolecule and water molecule in nanochannel need to be further researched. The transfer of biomolecule in nanochannel meanly includes two processes: (1) the pressure-driven flow of biomolecule in nanochannel; (2) the biomolecule permeating into nanochannel by pressure. First process needs to be researched, that is the pressure-driven flow of biomolecule in nanochannel. Therefore, unbalanced molecular dynamics and GROMACS were selected to research the pressure-driven transfer characteristic of biomolecule and water molecule on glass walls of nanochannel.

Silicon dioxide nanochannel model needed to be built in the preprocessing stages of GROMACS. Then biomolecule was added

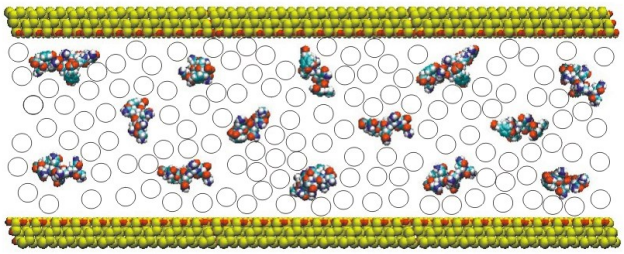

Figure 2. Schematic diagram of the SiO_2 nanochannel model, two silica walls are on the top and the bottom, many proteins are located between the top and the bottom wall.

into nanochannel, next water was done. Final, a certain ion was added into system according to the charged property of system, the purpose was to the electric neutrality condition of system. The final building model was shown in fig.2. As shown in fig.2, Y and X directions were defined as channel height direction and the channel direction, respectively. Protein molecules, Na^+ and Cl^- were distributed evenly in the channel.

The crystal face of β quartz crystal (111) was selected to simulate the face of silicon dioxide. Through MS Modeling and programming software, silicon dioxide nano channel was obtained as shown in fig.2. The faces with hydrogen atom on the two side of channel were exact opposite. The channel size: L_X:L_Y:L_Z=26.918: 10.438: 9.420nm.Water molecule model was SPC/E (simple point charge) model. Relatively simple polypeptide GNNQQNY was selected to simulate protein molecules. The protein molecules were added into channel randomly in the process of simulation. The number of protein molecules was used to maintain the constant protein concentration and the protein concentration in system was 0.03M. Rectangular unit bulge was used to simulate minimum rough element, modeling for rough wall.

Charmm27 force field in GROMACS 4.5 was selected as force field and the wall model was adopted. A harmonic potential was exerted on every molecule on wall surface on the interface of fluid and solid, which fixed every molecules on the wall surface on its lattice position by harmonic spring. The elastic potential energy expression was the following Eq(1).

$$u_{wall}\left(\left|r\left(t\right)-r_{eq}\right|\right)=\frac{1}{2}K\left(\left|r\left(t\right)-r_{eq}\right|\right)^2 \tag{1}$$

Where *r (t)* is the atom position at t time, r_{eq} is the primary atom lattice position, *K* is elasticity constant.

Directly imposing acceleration on fluidic molecules and biomolecules in channel was to simulate the real pressure-driven. The force condition of every fluidic molecule changed due to the acceleration and the force equation of fluidic molecules was calculated as Eq(2):

$$F_{fluid}\left(r_i\right)=\sum_{j=1}^{N_f}\frac{\partial V\left(r_{ij}\right)_{fluid-fluid}}{\partial r_{ij}}+\sum_{j=1}^{N_w}\frac{\partial V\left(r_{ij}\right)_{fluid-wall}}{\partial r_{ij}}+m_i a \tag{2}$$

Where N_f is the number of fluidic molecules at the connection with molecules within the cut-off radius, N_w is the number of wall molecules at the connection with molecules within the cut-off radius, m_i is the mass of the i^{th} fluidic molecule, α is the imposing acceleration. In the equation, the first part is the interaction force between fluidic molecules and surrounding fluidic molecules. The second part is the interaction force between fluidic molecules and surrounding solid wall molecules. The third part is external force. Due to the introduction of elastic potential energy, the force condition of wall molecules also changed. The force equation is show as Eq(3).

$$F_{wall}\left(r_i\right)=\sum_{j=1}^{N_w}\frac{\partial V\left(r_{ij}\right)_{wall-fluid}}{\partial r_{ij}}+k\left|r_0-r_j\right| \tag{3}$$

Where *k* is the elastic constant of harmonic potential exerted on wall, r_0 is the position of wall crystal lattice, r_j is the current position of molecules on wall surface. In the equation, the first part is the interaction force between molecules on wall surface and surrounding fluidic molecules. The second part is the elastic force exerting on molecules on the wall surface.

3. EXPERIMENTAL

The UV photolithography and wet etching technique were applied to fabricate the nano channels on the glass substrate. The relative effects of the etchant component, etching time, temperature and mask thickness on the depth as well as shape of the nano channels were investigated and analyzed systemically. Then the substrate and PDMS were bonded at room temperature. A minimum channel depth of 50mm was achieved. A profilometer was used to measure the depth of the initial channel before bonding. With the SEM images, nano channel shapes have been demonstrated.

3.1. Material and equipments

The reagents and materials involve sodium hydroxide, concentrated sulfuric acid, acetone, hydrofluoric acid, ammonium fluoride, nitric acid, perchloric acid (all analytical reagent). Ultrapure water was used. The SG2506 substrate (62×62cm^2) was purchased from Changsha Shaoguang Microelectronics Corp. The devices involved a 90005-02C ultrapure water system (LABCONCO, Corp.), a BS110S electronic balance (BSISL, Corp.), a JKG-2A lithography machine (Shanghai Xueze Optical Machinery Corp.)a PDC-32G Gas plasma Dry cleaner(Harrick Scientific Corp.), a KW-4A spin coater (Institute of Microelectronics of Chinese Academy of Sciences), a ultrasonic cleaner KQ5200DB(Kun Shan Ultrasonic Instruments Corp.), a ZTX3E stereoscopic microscope (Ningbo Huaguang Precision Instrument Corp.) and a DHG-9030A electrothermostatic blast oven(Shanghai Jing Hong Laboratory Instrument Corp.).

3.2. Chip fabrication

In this work, CorelDRAW12.0 was used to design the masks for the nano channels, With L-EDIT, the nanofluoidic channels was designed as shown in fig.3.

The substrate was spin coated with Cr (145nm) and AZ-1805 positive photoresist (550nm). After a quick exposure to the ultraviolet radiation, the substrate was developed in the NaOH (0.5%) solution for about 40s. Then the developed substrate has to be washed in the ultrapure water. Next, the chip was heated in the drying machine at 110ºC for 15min. A solution of 70%$KClO_4$

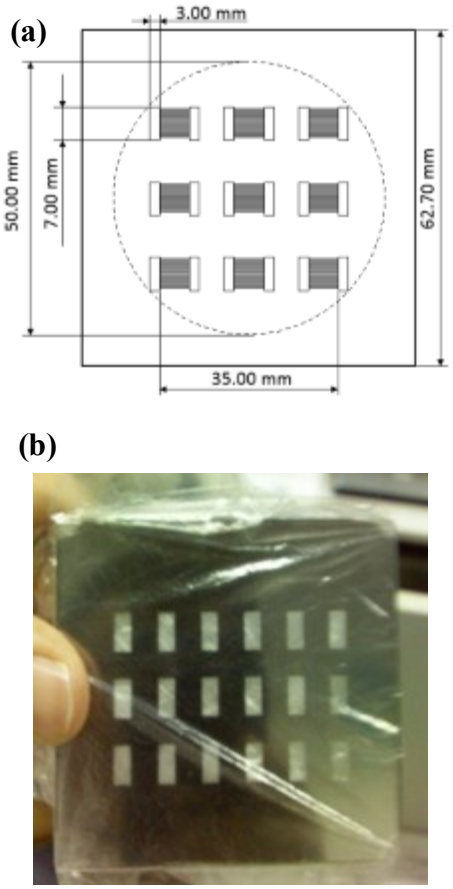

Figure 3. Design and fabrication of the mask (a) design of the mask with CorelDRAW12.0 (b) the fabricated mask

Figure 4. Etched glass chip

+$(NH_4)_2Ce(NO_3)$+H_2O was used to wipe out Cr for 2min till the channels appears. About 25-30ml corrosive liquid (1mol/L HF:1mol/L NH_4F) was used along with a mini-shakers for 30min, and a channel with a 20um depth and 40um width was obtained. Anhydrous ethanol was then used to wipe out the photoresist, then the Cr layer was washed up.

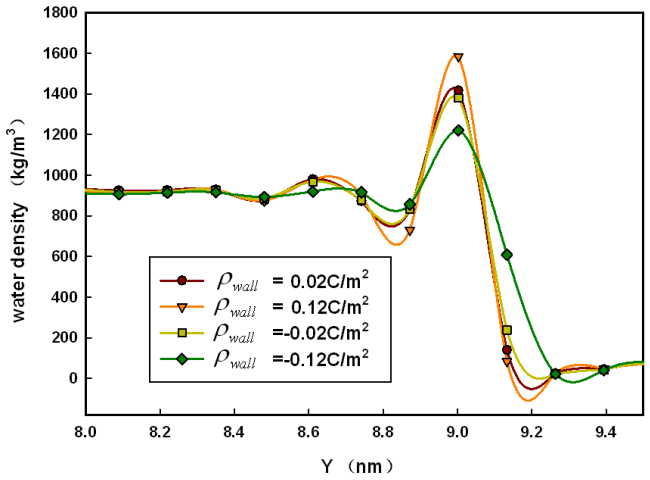

Figure 5. Contrast of the water density distribution under different wall charge density

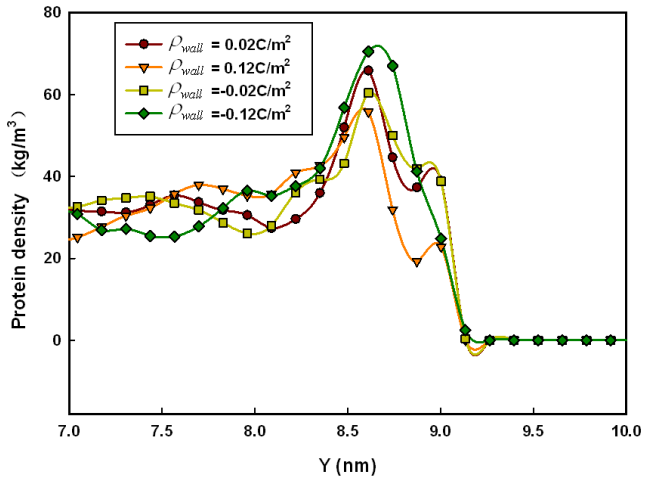

Figure 6. Contrast of the protein density distribution under different wall charge density

Anodic bonding technique is used. A mixture of PDMS and its curing agent (10:1), well prepared by ultrasonic, was first squeezed in a custom-designed molding block and then cured for 30min at 75ºC. The next stage for the fabrication of the nanofluidic chip was to seal the microfluidic channels so that the fluid could flow through the nanofluidic region confined by the nanochannels arrays. Before sealing, with cover slip, the glass substrates were mechanical drilled through the backside to access the inlets and outlets. The bonding step was realized between the superior PDMS layer and the inferior glass substrate. After oxygen plasma activation of their surfaces in plasma cleaner (PDC-32G-2) to enhance the surfaces wettability, wafers were aligned and then brought in contact. The bonding immediately happened just after the contact.

4. RESULTS AND DISCUSSION

4.1. Simulation results and channel optimization

Wall charge density mainly affect fluid density distribution near the wall, but has little effect on the fluid velocity. The effects of

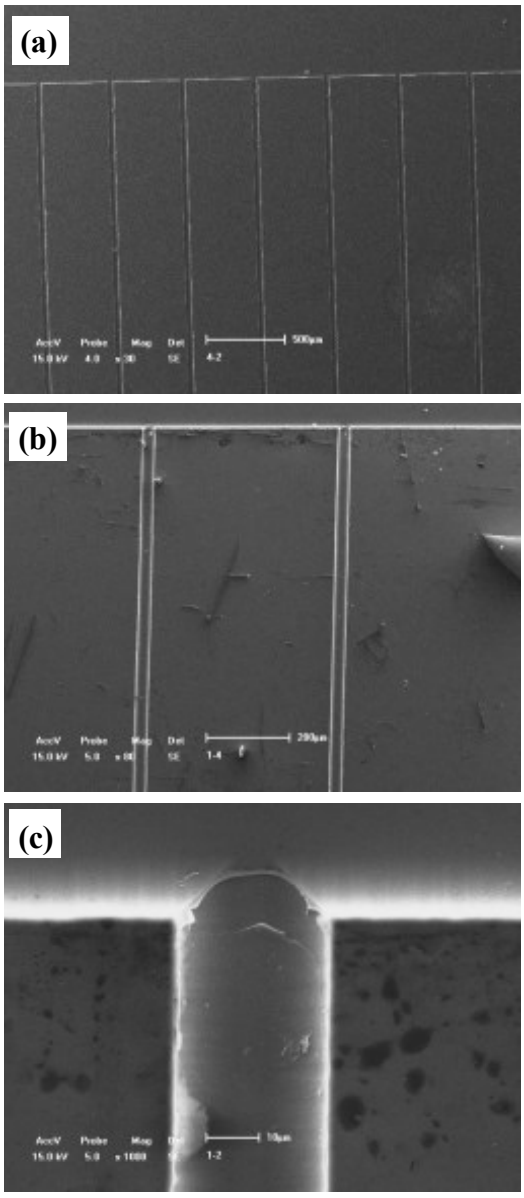

Figure 7. Effect observed by SEM after etching(a) 30 times magnification(b) 80 times magnification(c)1000 times magnification

wall charge density on water and protein density distribution were discussed. In the simulation, wall charge density was changed while keeping other parameters constant, the channel height h was set to be 8.5 nm, the accelerated speed was set to be 5 nm/ps^2, the temperature was set as T=300 K, the roughness was set as $R_{surface}$=1. The water and protein density distribute uniformly in the middle part, the wall charge density significantly affect the density near the wall, and the contrast of the water density distribution was shown in fig.5.

The height of wall was set as Y=9.35 nm, the peak density near the upper wall at Y=9 nm. As can be seen in fig.5, the peak density decreased from 1587 to 1428 kg/m^3 with the decrease of wall charge density from 0.12 to 0.02 C/m^2, when the wall charge density decrease to a negative value -0.12 C/m^2, the peak density decreased to 1219 kg/m^3.

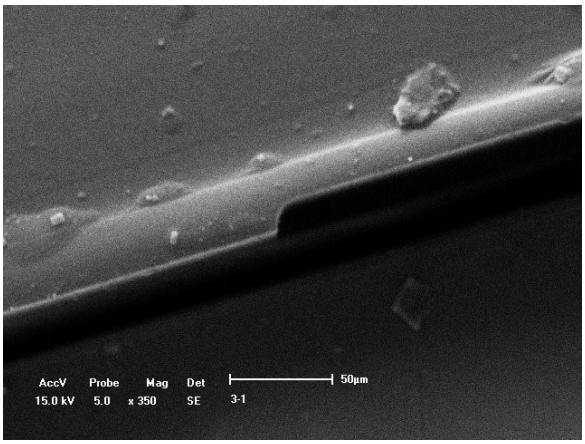

Figure 8. Channel map observed by SEM after sealing

Due to the different mass number between the hydrogen atom and oxygen atom, the water density near the wall decreases with the decrease of wall charge density. When the wall is positively charged, the negatively charged oxygen ions in water increased with the wall charge density. In contrast, the adsorbed hydrogen ions decrease, which leads to an increase of the peak density. When the wall is negatively charged, the positively charged hydrogen ions increased with the wall charge density while the peak density decreases.

The contrast of the protein density distribution under different wall charge density was shown in fig.6. When the wall charge density varies with at 0.12, 0.02, -0.12 and -0.02 C/m^2, the peak density stops uprising and drops accordingly at 8.57, 8.60, 8.61 and 8.66 nm while the corresponding density is 56, 60, 65 and 71 kg/m^3 respectively.

As can be seen, with the decrease of wall charge density, the peak location is nearer to the wall, the peak density increases. The protein molecule is positively charged, when the wall is positively charged, the repulsive force between the wall and protein molecule decreases with the wall charge density. When the wall is negatively charged, the attractive force between the wall and protein molecule increases with the wall charge density. Both the decreasing repulsive force and increasing attractive force lead to a nearer location from the wall and the increasing of the peak density.

4.2. Topography characterization of channel

Scanning electron microscope (SEM) is one of the most direct means in studying the material structure. The etched channels was characterized by SEM, then the channel width and the cross sectional image were showed in fig.7.

The channel contour and arrangement can be seen clearly in fig.7a and fig.7b. It notes that evenly distributed microarray channels were obtained by lithography-etching technical process. fig.7 (c) showed the microstructure on the channel surface, the effects of surface structure need to be considered in the model. The channel map after sealing observed by SEM was shown in fig.8. It can be seen that the edge sealing effect was good with no collapse.

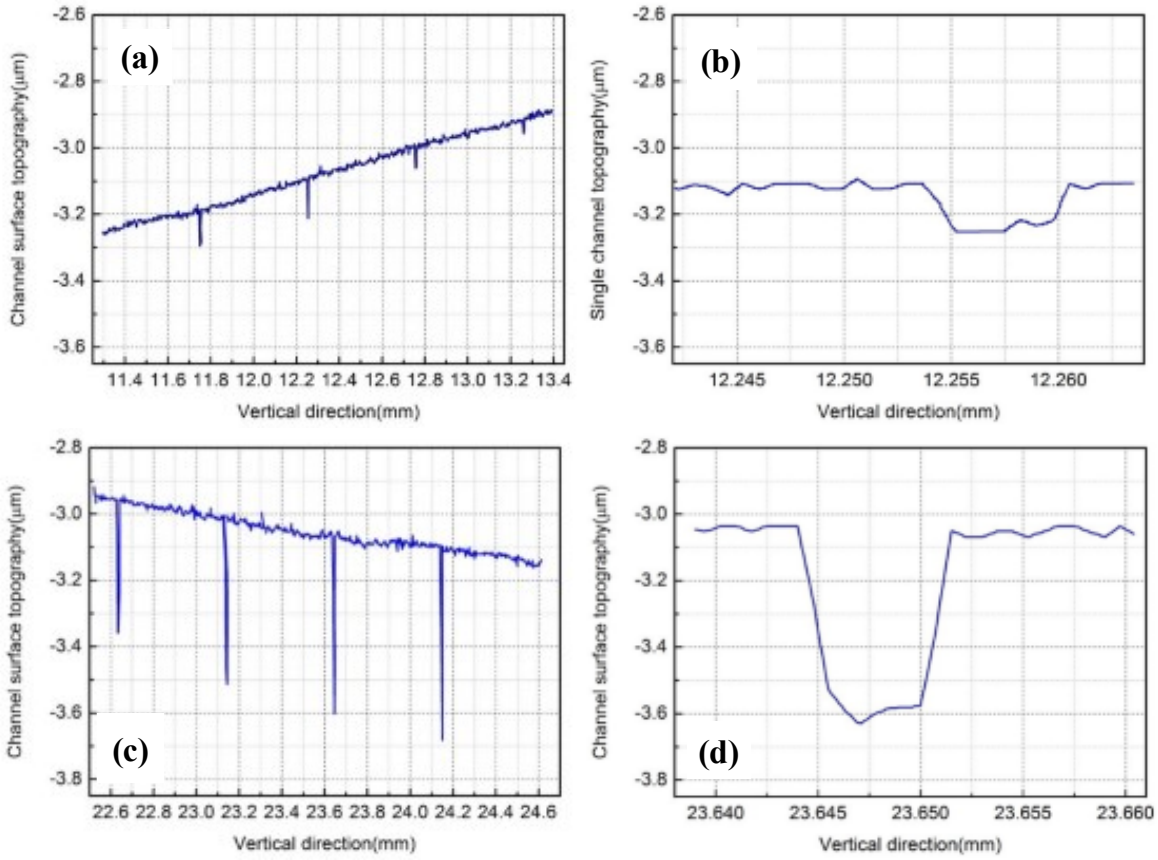

Figure 9. Channel topography characterized by high resolution roughness profilometer: (a) channel arrays of target depth at 100nm; (b) single channel of target depth at 100nm; (c) channel arrays of target depth at 500nm; (d) single channel of target depth at 500nm

4.3. Nanochannels characterization

The surface of intact grooves was complex, and the etching depth was uneven rectangle, the samples with etching depth at 100 nm and 500 nm were characterized along the vertical direction by high resolution roughness profilometer, the channel topographies were shown in fig.9.

The profilometer measured the depth of the nanochannels. As can be seen from fig.9a and fig.9b, with a suitable etching time, the nanochannels with depth at 78-112 nm would be obtained. In fig.9c and fig.9d, with the extension of etching time, the nanochannels with depth at 510-620 nm would be obtained. The characterized nanochannels with clear coutours met the design requirement.

4.4. Depth and etching time

Etchant, etching temperature and stirring method directly affect the etching rate and surface quality in wet etching process. Hydrofluoric acid with lead fluoride is normally used as glass etchant. When the channel width were 2 μm, 5 μm and 10 μm, the depth varied with different etching time was shown in fig.10.

As can be seen in fig.10, the channel depth is directly proportional to the etching time. When the etching depth is large, as micropump, microvalve and so on, the photoresist and chromium layer have a long soak in the etchant, it demands a higher etching rate to prevent the destruction. When the etching depth is little, as cap

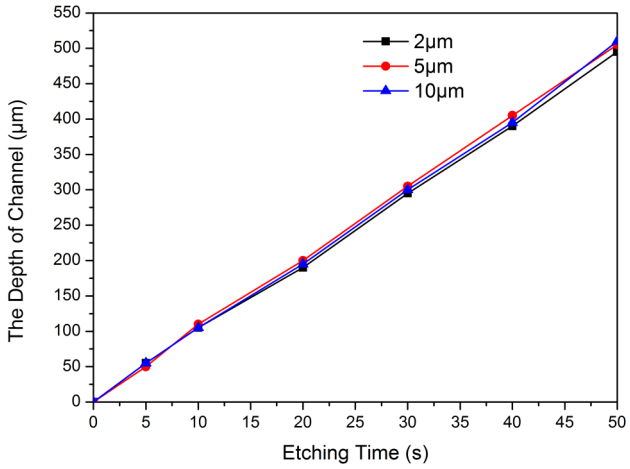

Figure 10. Variation of the depth of channel changing with time

illarypaths in electrophoresis chip, channels in micro mixer and so on, it demands a higher surface quality. Thus, the characteristic of the manufacturing object determine the etching condition, the etchant element and ratio, especially the latter.

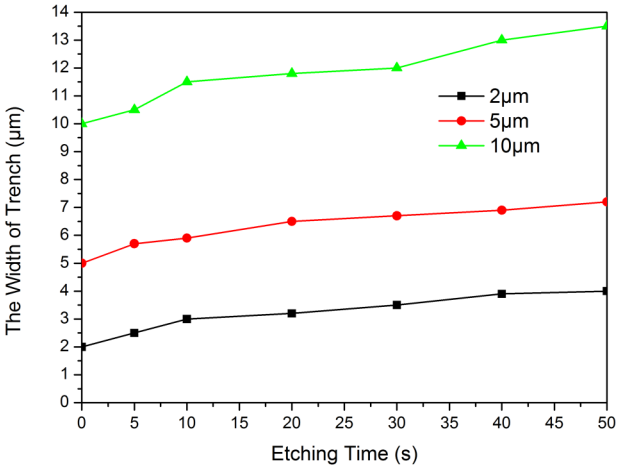

Figure 11. Variation of the width of trench changed with etching time

The etching direction was not downward in the whole process, the nanochannels with width at 2 μm, 5 μm and 10 μm were tested by profilometer, the effect of etching time on nanochannel width was shown in fig.11.

5. CONCLUSIONS

Based on electrical properties of nanochannel diode and electrochemical effect of nanofluidic channel, the glass microfluidic chip was designed and simulated using molecular dynamic, molecular simulation of the nanochannel model was achieved by GROMACS software, by using proteins as biomolecules, the effect of wall charge density on protein density was studied. In this work, nanofluidic chip with width at 2 μm, 5 μm and 10 μm were obtained by wet etching and room temperature bonding technique, and characterized by SEM and roughness profilometer. Nanofluidic chip with minimum depth at 100 nm with no collapses at 100 nm to 500 nm was obtained, the edge sealing effect was good. we also studied the effect of etching time on channel width and depth. Based on electrochemical effect, the design method for nanofluidic channels in this work offeres a significant exploration for nanofluidic technology.

6. ACKNOWLEDGMENTS

This work is jointly supported by National Natural Science Foundation of China (51376039), Doctoral Fund of Ministry of Education of China (20120042110031) and the Fundamental Research Funds for the Central Universities of China (N120403006, L1503004).

REFERENCE

[1] Rohit Nandkumar Karnik. Manipulation and Sensing of Ions and Molecules in Nanofluidic Devices[D]，University of California, Berkeley, 2004.

[2] Wang YC, Stevens AL, Han J., J. Anal. Chem., 77, 4293 (2005).

[3] Pu QS, Yun JS, Temkin H. et al., Nano Lett., 4, 1099 (2004).

[4] Garcia AL, Ista LK, Petsev DN et al., Lab Chip J., 5, 1271 (2005).

[5] Sivanesan P, Okamoto K, English D et al., Anal. Chem., 77, 2252 (2005).

[6] Han J, Craighead HG., Science, 288, 1026 (2000).

[7] Dukkipati VR, Kim JH, Pang SW et al., Nano Lett., 6, 2499 (2006).

[8] Kaji N, Tezuka Y, Takamura Y, Ueda M, Nishimoto T, Nakanishi H, Horiike Y and Baba Y, Anal. Chem., 76, 15 (2004).

[9] Fu JP, Han J, Micro Total Analysis Systems, 1, 285 (2005).

[10]Cipriany BR, Craighead HG, Automated Single Molecule Selection, Ieee International Electron Devices Meeting (Iedm), 2011.

[11]Patrick J. Murphy, Benjamin R. Cipriany, Christopher B. Wallin et al., PNAS, 110, 7772 (2013).

[12]JS Varsanik, JJ Bernstein, Micromechanics and Microengineering, 23, 95017 (2013).

[13]Schoch RB, Bertsch A, Renaud P, Nano Lett, 6, 543 (2006).

[14]Wu JZ, Jiang T, Jiang, D.E. et al., Soft Matter., 7, 11222 (2011).

[15]Andersen MB, Frey J, Pennathur S et al., Journal of Colloid and Interface Science, 353, 301 (2011).

[16]A. Plecis, C. Nanteuil, Anne Marie Haghiri Gosnet and Y. Chen, Anal. Chem., 80, 9542 (2008).

[17]Kuo T., Analytical Chemistry, 75, 1861 (2003).

[18]Daiguji H, Yang P, Majumdar A, Nano Letters, 4, 137 (2004).

[19]Karnik R, Castelino K, Majumdar A, Applied Physics Letters, 88, 123114 (2006).

[20]Neumann J. Hennig M, Wixforth A et al., Nano Letters, 10, 2903 (2010).

[21]Rajauria S., Axline C., Gottstein C. et al., Nano Letters, 15, 469 (2015).

[22]Wright G, A Costa L, Terekhov A et al., Microscopy and Microanalysis, 18, 816 (2012).

[23]Takayama S, Huh D, Song J et al., Micro- and Nanofluidics for Cell Biology, Cell Therapy, and Cell-Based Drug Testing, Icnmm, Pts a-B:1395 (2009).

[24]Hodko D, Raymer L, Herbst SM et al., Biomedical Instrumentation Based on Micro- and Nanotechnology, 2, 65 (2001).

[25]Arayanarakool R., Shui L.L., Kengen S.W.M. et al., Lab on a Chip, 13, 1955 (2013).

[26]Parikesit Gea O., Kutchoukov Vladimir G., van Oel Wim et al., Proceedings of the SPIE, 5515, 109 (2004).

[27]Gerspach M.A., Mojarad N., Pfohl T. et al., Microelectronic Engineering, 145, 43 (2015).

[28]Napoli M, Eijkel J.C.T, Pennathur S., Lab on a Chip, 10, 957 (2010).

[29]Zhang C. Zhang F. van Kan J.A. et al., Chemical Physics, 128, 185103 (2008).

[30]Balducci A. Mao P. Han J.Y. et al., Macromolecules, 39, 6273 (2006).